Chapter 6

Co-cultivation strategy using *D. mucosa VSPA* and *Scenedesmus obliquus* for enhanced biomass production and bioremediation

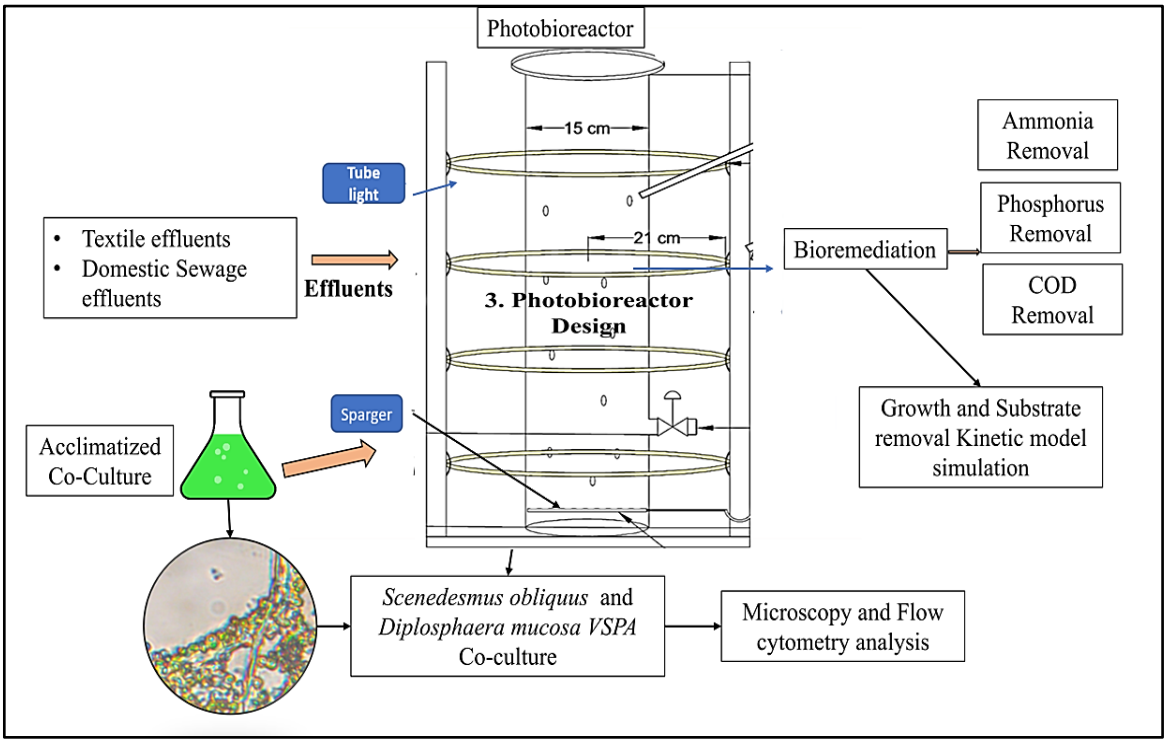

Cocultivation of *D. mucosa VSPA* and *Scenedesmus obliquus* for enhanced biomass production and bioremediation

6.1. Introduction

In the current investigation, a newly isolated strain from the inlet of the sewage treatment plant and *S. obliquus* were co-cultivated to treat Textile Effluent (TE) and Domestic effluent (DE). Treatment was performed in a conventionally designed 10-liter bubble column photobioreactor. The co-cultivation mode was evaluated by comparing biomass production, and nutrient removal with the mono-cultivation mode using heterotrophic and mixotrophic cultivation modes. The change in the population of both strains during co-cultivation was analysed by microscopy and flow cytometry.

6.2. Materials and methods

6.2.1. Culture Procurement and its Maintenance

Microalgal species *S. obliquus* (NCIM 5586) was procured from the National Collection of Industrial Microorganisms (NCIM), National Chemical Laboratory (NCL), Pune. The strain was obtained on slants and revived in Bold Basal Media (BBM) [361]. Cultures were revived in 250 ml flasks with 100 ml sterilised BBM media and kept in a shaking incubator at 25°C with a shaking speed of 120-rpm. Flasks were illuminated by LED tubes at 2500 lux intensity with a duration of 16:8 hours of light/dark cycles. pH was monitored daily and adjusted to pH 7 using 1 N NaOH and 1 N HCl. The flasks were covered with non-absorbent cotton plugs for capturing ambient CO_2. The culture was allowed to grow in the above-mentioned conditions until the exponential phase was achieved (3–5 days of cultivation). Subculturing was done every 30 days, and culture from the exponential phase was further used for the study.

6.2.2. Culture Isolation and Identification

The second strain was isolated from samples taken from the inlet of the sewage treatment plant (STP) located at Bhagwanpur, Varanasi, India (25.27, 83.00). A ten-fold serially diluted sample was spread over BBM agar plates. Plates were illuminated by LED tubes at 2500 lux intensity with a duration of 16:8 hours of light/dark cycles, kept at 25^{o}C in an incubator. Individual colonies were picked and further purified by repeated streaking. The purity of the culture was confirmed by observing it under the microscope. The isolated culture was named VSPA and identified by 18s rRNA sequencing. NCIM, NCL Pune, India, assisted with the sequencing process. Chromosomal DNA was isolated using a spin column kit (HiMedia, India), and after that, amplification of the 18s rRNA gene (1500 bp) was done using polymerase chain reaction (PCR) in a thermal cycler. After PCR, purification was done using exonuclease I-shrimp alkaline phosphatase (Exo-SAP). Sanger's chain termination method was used for sequencing the purified amplicons in the ABI 3500XL genetic analyzer (Life Technologies, USA). CHROMASLITE (version 1.5) is used for editing the obtained sequencing files. The BLAST (Basic Local Alignment Search) tool that finds regions of local similarity between sequences was used to find the most similar and closest sequence from the obtained sequence at the National Center for Biotechnology Information (NCBI). Similar sequences obtained through the BLAST tool were used for the phylogenetic tree construction using MEGA (version:11) with the bootstrap value of 100.

6.2.3. Inoculation ratio determination

To determine the best inoculation ratios for cultivating both strains, VSPA and *Scenedesmus* were cultivated in the ratios of 1:1, 1:2, 1:4, 1:8, and 1:16 in BBM [362]. Both species were also cultivated in monoculture mode as a control. The cultivation

conditions were kept the same as during the revival of the culture. The best inoculation ratio was then further used for the next experimental designs.

6.2.4. Wastewater collection and characterization

Two types of effluents, TE and DE, were treated in co-cultivation mode. TE was collected from local industries located in Varanasi. DE was collected from the Assi River, which flows through the majority of Varanasi's southern areas. The Assi river is mainly polluted by DE flowing from households in Varanasi. The temperature of the effluent was measured using a mercury thermometer at the collection site. After that, samples were pre-treated via filtration and sedimentation and stored at 4^{o}C for further use. Sample characterization was performed following internationally recognised procedures as mentioned in APHA [363].

6.2.5. Experimental Design

The experimental design of the current research is shown in **Table 6.1**. Six experimental runs were carried out in order to compare co-cultivation and mono-cultivation modes in both heterotrophic and mixotrophic modes.

The co-cultivation mode's efficiency was evaluated by co-cultivating both species at the best inoculation ratio. The mono-cultivation mode was carried out as a control. The effluents were treated in both modes in batch experiments performed in conventionally designed cylindrical PBR. The reactor was made up of an acrylic tube with a total height of 60 cm and inner and outer diameters of 15 cm and 17 cm, respectively. The total reactor volume was 10.6 L, and the working volume was 9 L.

Each experiment was also performed in heterotrophic and mixotrophic modes. Each batch was inoculated with 10% (v/v) inoculum from both cultures when the mid-log phase was reached. The treatment was continued for ten days until the stationary phase was reached. Continued aeration at a rate of 3 L/min of air was provided using an air compressor pump. For mixotrophic mode, two 30 W LED tube lights placed opposite each other were

used for the illumination of PBR, providing a light intensity of 4500 lux and maintaining 12h:12h light and dark cycles. Lights were turned off entirely during the heterotrophic mode of cultivation. Rest parameters were similar to those used during the revival and isolation of the culture. Following the completion of each experimental run-in triplicate, the average data with standard deviation was used for further calculation.

Table 6.1. The experimental design used in the current co-cultivation study.

Run	**Strain**	**Cultivation Mode**	**Culture Mode**	**Light Source**
1	VSPA	Mono-cultivation Mode	Heterotrophic Mode	Not Supplied
2	*S. obliquus*	Mono-cultivation Mode	Heterotrophic Mode	Not Supplied
3	VSPA + *S. obliquus*	Co-cultivation Mode	Heterotrophic Mode	Not Supplied
4	VSPA	Mono-cultivation Mode	Mixotrophic Mode	Supplied
5	*S. obliquus*	Mono-cultivation Mode	Mixotrophic Mode	Supplied
6	VSPA + *S. obliquus*	Co-cultivation Mode	Mixotrophic Mode	Supplied

6.2.6. Flow cytometry and microscopic analysis

For microscopic analysis, 1 µl of the culture was fixed on a glass slide and protected by a cover slip. Following that, glass slides were examined under a microscope with a resolution of 40X. Next, flow cytometry analysis was performed via CytoFLEX, Beckman Coulter (USA). 1 ml of the sample was diluted in the 2 ml phosphate buffer. Then the solution was filtered through a 35µm filter vial to avoid clogging the instrument. The filtered sample was used for the flow cytometry analysis. Initially, daily cleaning of the instrument was performed using a cleaning buffer, and then quality control standardisation was done using standard solutions. Samples containing unstained cells were placed into the inlet of the flow cytometry device. A sample was moved at a flow rate of 30 L/min by a sheath fluid (0.1% 2-phenoxyethanol) via a laser light beam of a 405nm (violet) wavelength. Forward-scattered light (FSC) and side-scattered light (SSC) signals from a violet laser were detected by an avalanche photo diode detector. The sample experiment was performed at 10,000 events that were recorded. The monoculture cells were analysed before the co-cultivation analysis, and the population of microalgal cells in monoculture and co-cultivation modes was designated as a circle gate. Cytexpert software was used for the analysis of co-cultivation results.

6.2.7. Kinetic Modeling of Microalgal Growth and Substrate Removal

To simulate any biological process, suitable growth and substrate removal kinetic models need to be developed. Such models are very generous for designing and improving large-scale reactors used in effluent treatment plants [364]. In this study, the experimental results (data) were successfully fit to the sigmoidal curve models that are described below.

6.2.7.1. Logistic growth kinetics model

Using the logistic model, you can figure out how the growth rates of microalgal species change over time. The logistic growth model is not affected by substrate concentration [365]. According to the logistic growth model, the microalgal-specific growth rate is inversely correlated with the microalgal biomass concentration. [366]. It defines endogenous and exponential metabolic phases [367]. Therefore, microalgal growth has been described in Eq. (6.1) [368]:

$$\frac{dX}{dt} = \mu_m X\left(1 - \frac{X}{X_m}\right) \quad (6.1),$$

where X denotes the concentration of biomass (g/L) at time t(d), X_m is the maximum concentration of biomass (g/L), and μ_m is the maximum specific growth rate (d^{-1}). Integration of Eq. (1) yielded Eq. (6.2):

$$X(t) = \frac{X_0 X_m e^{\mu_m t}}{X_m - X_0 + X_0 e^{\mu_m t}} \quad (6.2),$$

where X_0 denotes the initial biomass concentration (g/L) (at, t = 0) and X_m is the stationary biomass concentration. A sigmoidal-shaped growth profile with lag, exponential (log), and stationary phases is shown by the logistic growth kinetics model. [367].

6.2.7.2. Gompertz Model

After the logistic model, Gompertz's model is the preferred growth model used for growth kinetics. Gompertz's model has two types depending on the parameters (that are kept constant) either concerning the x or y-axis, respectively, the Type I model and the Type II model. In Type I, the values on the x-axis are influenced by a single parameter at a very precise point on the curve. In Type II, the initial value (intersection through the y-axis) is regulated by multiple parameters [369]. The Gompertz model was altered to explain the growth pattern, depending on the following assumptions: (i) follows first-order growth kinetics (growth declines and inclines exponentially); (ii) non-saturating substrate; and (iii)

the growth of biomass is proportionate to the dry biomass weight (W) as μ is constant. An improved Gompertz growth kinetics model has been shown in Eq. (6.3) [370], [371]:

$$X = A \times \exp\left[-exp\left\{\left(\frac{\mu_m \times \exp(1)}{A}\right) \times (\lambda - t) + 1\right\}\right] \quad (6.3),$$

where X represents the microalgal biomass concentration (g/L) at time t (day, d), μ_m denotes the maximum specific growth rate (d^{-1}), λ is the lag time (d), and A is the maximum biomass concentration (g/L). Eq. (6.3) is better known as the Type I Gompertz model. To determine the substrate removal rate, Eq. (3) was modified as Eq. (6.4) [370].

$$S(t) = S_i + (S_f - S_i) \times \exp[-\exp\{k \times (\lambda - t) + 1\}] \quad (6.4),$$

where S(t) represents the substrate or nutrient concentration (mg/L) at time t (d), S_i represents the initial substrate concentration (mg/L) at t = 0, S_f represents the final substrate concentration (mg/L), and k is the nutrient uptake rate or substrate utilisation rate (d^{-1}).

6.2.7.3. Substrate dependent/independent models

Two models, Model I and Model II, have been established by Murwanashyaka et al [364], built on the assumption that substrate assimilation can be independent of or dependent on microalgal growth [364]. Model I figured out the usual kinetic model, which defines that the biodegradation of organic matter can be used to estimate nutrient uptake patterns by microalgal cells. It imitates an absolute link between nutrient uptake and microalgae growth. Ideally, this model will estimate the nutrient uptake pattern at a finite concentration. The model I is also applicable to evaluate the maximum nutrient reserve content in the microalgae cells, which is a crucial criterion of interest while observing nutrient removal in effluent treatment [372].

Model II is based on first-order kinetics and assumes substrate assimilation is analogous to adsorption. It pretends that there is no link between microalgal cell growth and nutrient uptake. Additionally, Model II presumes that the microalgae cells execute a

chain of activities comprising transformation and transportation for nutrient uptake [364]. Models I and II are represented in Eqs. (6.5) and (6.6), respectively:

$$-\frac{dS_a}{dt} = k \cdot S_a \cdot X \quad (6.5)$$

$$-\frac{dS_a}{dt} = k\, S_a \quad (6.6),$$

where X is the microalgal biomass concentration (g/L) at time t (d), S_a is the substrate concentration that can be assimilated by microbes (mg/L), and k is the growth kinetic constant (d^{-1}). In the microalgal cultivation phase, the overall substrate concentration (S) is used in place of the assimilable substrate (S_a) for the experimental study. Consequently, the mathematical conversion of Eq. (6.5) produces Model I embodied by Eq. (6.7), as follows:

$$S = \frac{\left(\frac{X_o}{Y} + S_o\right)(S_o - S_{na}) + \frac{X_o}{Y} S_{na} exp(pt)}{(S_o - S_{na}) + \frac{X_o}{Y} exp(pt)} \quad (6.7)$$

Similarly, Eq. (6.6) generates Model II, denoted by Eq. (6.8), which calculates the changes in the substrate concentration pattern as follows:

$$S = S_{na} + (S_o - S_{na})\, exp(-k \cdot t) \quad (6.8),$$

where S_0 is the initial concentration of substrate (g/L), S_{na} is the non-assimilated substrate concentration (g/L), p denotes the maximum specific nutrient removal or substrate rate (d^{-1}), X_0 is the initial microalgal biomass concentration (g/L), and Y is the biomass yield coefficient (g/g).

6.2.7.4. Luedeking-Piret kinetics model

The parameters for both growth and non-growth-related product production are combined in the Luedeking-Piret growth kinetics model (Eq. 6.9):

$$q_p = \alpha \mu_g + \beta \quad (6.9),$$

where q_p symbolises the specific product formation rate, μ_g denotes the gross specific growth rate, α and β are the proportionality constant coefficients. If α = 0, it

signifies that product synthesis is not associated with growth, and if β = 0, it signifies that product formation is associated with growth [373].

Microalgae cells consume substrate mainly for product synthesis, cell maintenance, and cell growth. Although microalgal biomass is the main product, the utilisation of substrate assimilation for product formation was assumed to be neglected. On this basis, the Luedeking-Piret model was transformed to estimate substrate utilization. This model comprises the maintenance factor (m) (Eq. 6.10):

$$\frac{dS}{dt} = -\frac{1}{Y_x}\left(\frac{dX}{dt}\right) - mX \qquad (6.10)$$

The logistic model (Eq. (3)) was used to modify the Luedeking-Piret growth model as both models were based on almost similar hypotheses. Firstly, Eq. (6.10) is integrated. Then the integrated form of Eq. (6.10) and Eq. (6.2) was modified into Eq. (6.11):

$$S(t) = S_0 - \frac{1}{Y_x}\frac{X_0 X_m e^{\mu_m t}}{X_m - X_0 + X_0 e^{\mu_m t}} - m\frac{X_m}{\mu_m} ln\left(\frac{X_m - X_0 + X_0 e^{\mu_m t}}{X_m}\right) \qquad (6.11)$$

where S and S_0 denote the rate-limiting substrate concentration (mg/L) at time t (day, d) and the initial rate-limiting concentration of substrate (mg/L) at time t=0, respectively. X_0, X, and X_m denote the initial concentration of biomass (g/L), the biomass concentration (g/L) at any time t (d), and the final concentration of biomass (g/L), respectively, μ_m is the maximum specific growth rate (d^{-1}), m denotes the cell maintenance coefficient (d^{-1}), and Y_x represents the observed yield coefficient (g mg^{-1}) (Li et al., 2017).

6.2.8. Analytical Techniques

A fixed volume of the culture was withdrawn at a fixed interval of 24 hours during each run to determine nutrient and biomass concentrations. 5 ml of the sample was used for

determining the biomass concentration by taking absorbance at 680 nm and calculating the value using equations 6.12 to 6.14, respectively, for *S. obliquus*, VSPA, and strains cultivated during the co-cultivated mode. By plotting a standard curve between known biomass concentration and absorbance (680 nm), these equations were derived.

$$Abs. = 0.1324 \times Conc. \quad (6.12)$$

$$Abs. = 0.1402 \times Conc. \quad (6.13)$$

$$Abs. = 0.1556 \times Conc. \quad (6.14)$$

Next, to measure the nutrient level in the reactor, the remaining sample was centrifuged at 8,500 rpm for 15 minutes. The supernatant was collected for pollutant level analysis, and the pellet was used for microscopic analysis. Measurement of NH_4^+-N and PO_4^{3-}-P concentrations was carried out by spectrophotometric methods according to the phenate and vanadomolybdophosphoric acid methods, respectively [363]. The close reflux titrimetric method was used for measuring COD [363]. At last, the substrate removal efficiency (RE) was determined by Eq. (6.15), respectively:

$$RE = \frac{S_o - S_f}{S_o} \times 100 \quad (6.15),$$

where, S_o and S_f are the initial and final substrate concentrations (mg/L), and RE is the nutrient removal efficiency.

6.2.9. Statistical Analysis

All batch experiments were conducted in triplicate, and mean values were used for further calculation. All calculations and plotting were done using Origin Lab (Version 17). The student's paired t-test was performed using Origin Lab (Version 2017) to determine the significance of the results. Each test was considered significant at significance level of $p < 0.005$ (Probability value). The solver supplement of Microsoft Excel 2016 was used to execute non-linear regression to minimise the sum of squares error and determine the

model's kinetic parameters. To determine the model's goodness of fit, the coefficient of regression (R^2) was estimated.

6.3. Result and Discussion

6.3.1. Strain Identification

The molecular characterization of the isolated strain was done by 18s rRNA gene sequencing. A partial sequence of 1333 bp length was obtained by sequencing. Similar sequences were obtained by BLAST; and phylogenetic tree analysis was performed by MEGA 11 as shown in **Figure 6.1.** The analysis revealed that the strain has an 89.60% sequence similarity with the *Diplosphaera* genus and is closer to the *mucosa* species. Therefore, the strain was identified and named *Diplosphaera mucosa VSPA*. The strain belongs to the *Trebouxiophyceae* class and its nucleotide sequence has been submitted to GenBank with accession number ON599904.1. Notably, to the best of the author's knowledge, this is the first publication that reports the benefits of wastewater treatment by *D. mucosa* in the co-cultivation mode.

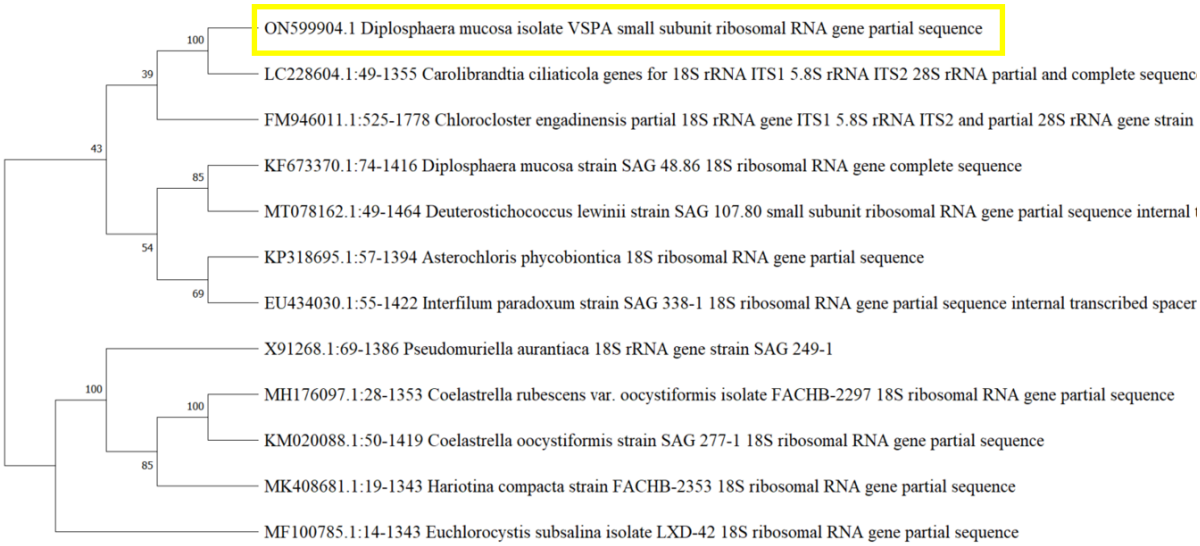

Figure 6.1. Phylogenetic tree (neighbour joining tree) construction using Mega11 software, with bootstrap value 100.

6.3.2. Effect of inoculation ratio

Before performing the effluent treatment in co-cultivation mode, it is necessary to determine the best inoculation ratio under which strain offers strong symbiosis. The stronger the symbiosis, the higher the biomass productivity. To determine the best inoculation ratio for co-cultivation, both strains were cultivated at different inoculation ratios, as shown in Table 2. Biomass productivity increased as the ratio was increased from 01:01 to 01:04, but afterward productivity decreased, as shown in **Table 6.2** and **Figure 6.2.** Also, the growth pattern under different inoculation ratios is represented in Figure 3. The highest biomass productivity was obtained at 01:04, which was 1.11 ± 0.01 g/L/day, with the final biomass concentration reaching 7.97 ± 0.08 g/L. The results can easily be interpreted as the co-cultivation mode surpassing the monoculture mode under all tested inoculation ratios. Results also show that both strains grow in symbiosis and support each other up to a specific limit, but after that, they start competing to consume the available nutrients.

Table 6.2 Effect of inoculation ratios on the symbiotic relationship between the two strains.

	Dip **(Hetero)**	***Sce*** **(Hetero)**	**01:01**	**01:02**	**01:04**	**01:08**	**01:16**
Biomass Concentration (g/L)	**4.64±0.20**	**4.18±0.09**	**5.45±0.02**	**5.45±0.02**	**7.97±0.08**	**6.93±0.09**	**5.49±0.05**
Biomass Productivity (g/L/day)	**0.61±0.03**	**0.52±0.01**	**0.66±0.03**	**0.73±0.00**	**1.11±0.01**	**0.85±0.05**	**0.65±0.02**

Dip: *D. mucosa*; *Sce*: *S. obliquus*;

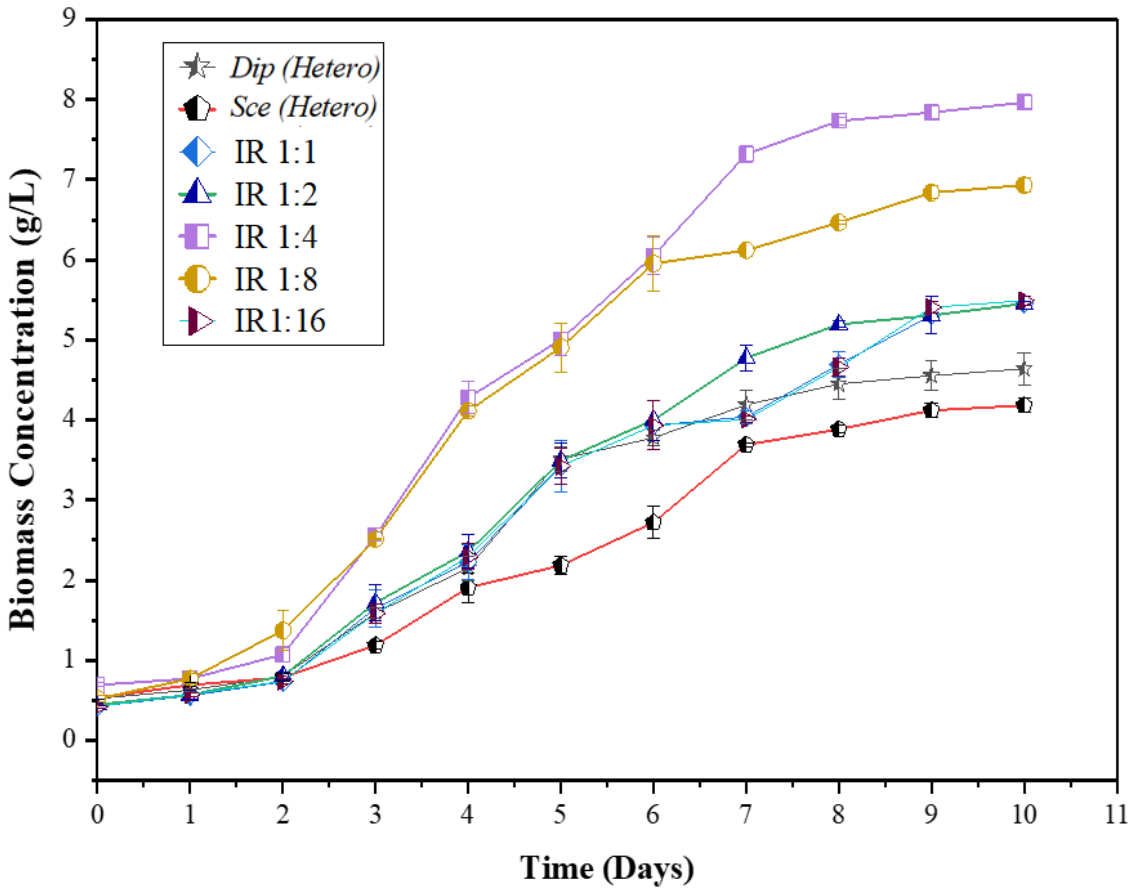

Figure 6.2. The pattern of growth of *Dip* and *Sce* strains in mono and co-cultivation mode under different inoculation ratios.

6.3.3. Microscopic and Flow Cytometry Analysis of Co-Cultivated Culture

The co-cultivated culture was further characterised by microscopic analysis and flow cytometry analysis. **Figure 6.3** represents the microscopic image of both strains cultivated in mono- and co-cultivation modes (01:04) in DE effluent. It can be observed from Figure 6.4 shows that *S. obliquus* grows in a thread-like structure formed when single cells fuse to form a row-like structure of 8 to 32 cells ("Phycokey - Scenedesmus," n.d.). While *D. mucosa* grows in single-celled mode, sometimes 4 - 8 cells may conjugate with each other [376]. During the co-cultivation mode, it was visible that the population of *D. mucosa* outnumbered *S. obliquus*, even though a high ratio of *S. obliquus* was supplied. It may be due to the high growth rate of *D. mucosa* as observed during experiments.

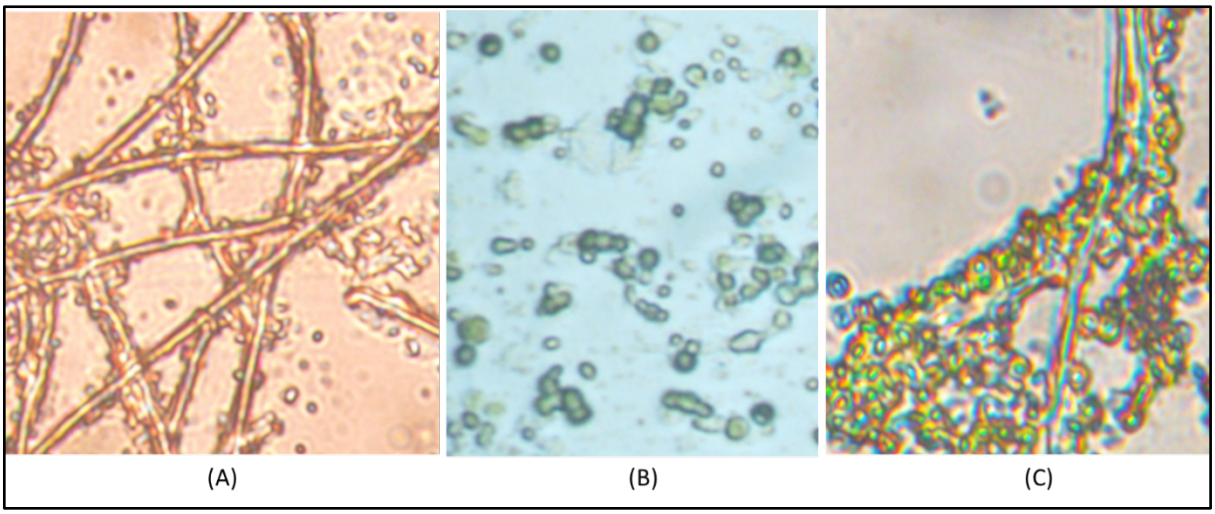

Figure 6.3. Microscopic image of cultures of (a) *S. obliquus*, (b) *D. mucosa*, and (c) co-cultivated culture during cultivation in DE effluent.

In addition to microscopic results, the symbiotic relationship between *D. mucosa* and *S. obliquus* can be analysed in a detailed manner by flow cytometry. Figure 5 represents the results of all events for both the strains cultivated in mono- and co-cultivation modes.

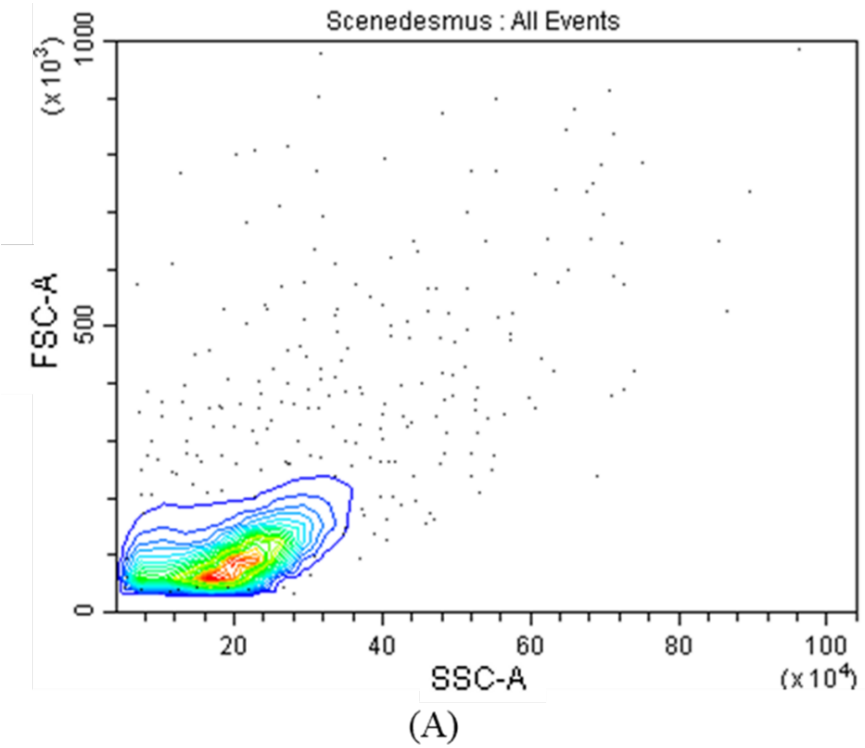

(A)

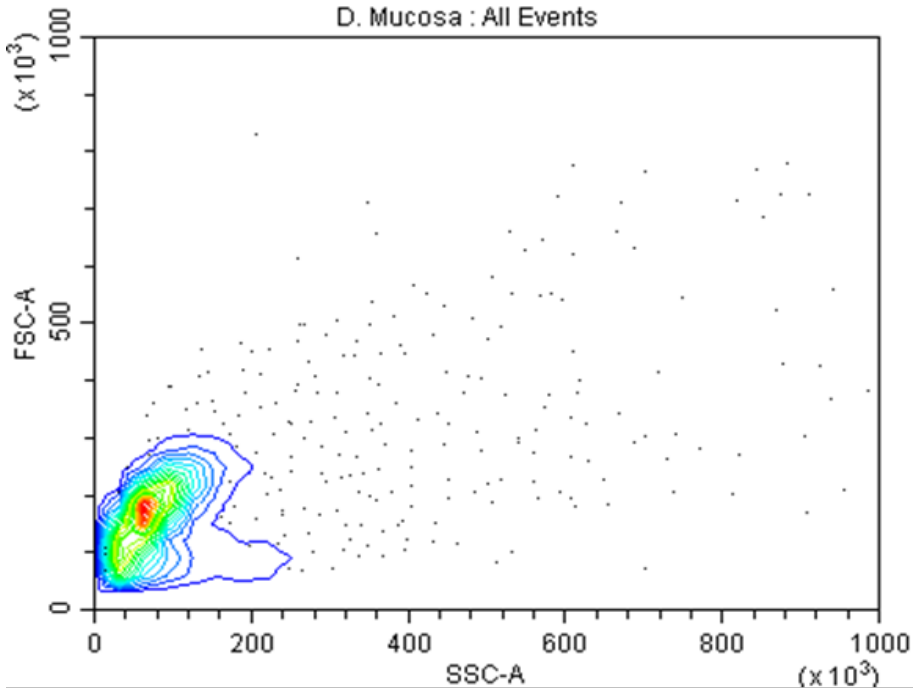

(B)

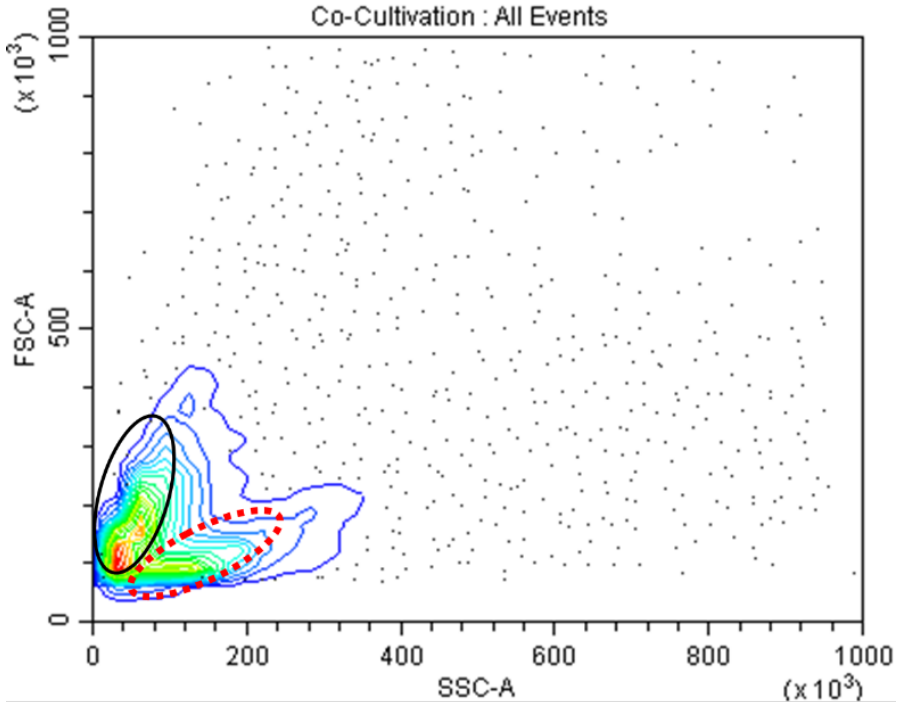

(C)

Figure 6.4. Flow cytometry analysis of (a) *S. obliquus*, (b) *D. mucosa* VSPA, and (c) co-cultivated culture (*D. mucosa* VSPA cells are encircled in a solid line and *S. obliquus* in a dashed line).

The contour plot of flow cytometry represents the cell density of the mono-cultivation mode. Figure 6.5(a) illustrates the *S. obliquus,* and Figure 6.5(b) represents the *D. mucosa VSPA*. In the co-cultivation contour plot, the solid line circle represents the *D. mucosa* VSPA strain, and the dotted line circle represents the *S. obliquus*. Figure 6.5(c) represents that plot being more concentrated towards the *D. mucosa* strain, indicating that the *D. mucosa VSPA* strain grows at a rate, outnumbering the population of *S. obliquus*.

6.3.4. Treatment Process in Co-Cultivation Mode

After determining the best inoculation ratio, DE and TE were treated in co-cultivation mode with an 01:04 inoculation ratio in both heterotrophic and mixotrophic modes. Mono cultivation mode acted as a control. The initial concentration of substrates or pollutants present in the effluent has been represented in **Table 6.3,** obtained after the characterization of effluents through standard procedures. A detailed analysis of biomass productivity and substrate assimilation has been discussed in the next section.

Table 6.3. Characterization of textile and domestic effluent through standard procedures.

S.No.	Parameter	Textile effluent	Domestic effluent
1.	pH	8.2	7.3
2.	Temperature (°C)	35	38
3.	TSS (mg/L)	430	940
4.	TDS (mg/L)	1350	980
5.	Total Solids (mg/L)	1780	1920
6.	Turbidity (NTU)	14.3	160
7.	Chloride (Cl^-) mg/L	660	685
8.	Alkalinity (carbonate)(mg/L)	52.8	76.8
9.	Phenol (mg/L)	3.8	1.84
10.	Nitrogen (ammonia)(mg/L)	54.6	89.8
11.	Nitrogen (Nitrate)(mg/L)	2.12	25.2
12.	Phosphate (mg/L)	6.3	7.8
13.	N/P ratio	8.6	11.51

14.	DO (mg/L)	1.6	1.8
15.	BOD_5 (mg/L)	87.2	135
16.	COD (mg/L)	372	520
17.	Total organic carbon (TOC)(mg/L)	164	264
18.	Color (Hazen)	180	220

TDS: Total dissolved solids; DO: Dissolved Oxygen; TSS: Total suspended solids;

6.3.4.1.Biomass production

The resource recovery of the current treatment process was accessed in terms of microalgal biomass. Microalgal biomass itself is a valuable resource as it can be further transformed into biofuel, biofertilizers, and bioethanol. **Figure 6.5** and **Table 6.4** represent the comparative evaluation of biomass production in mono- and co-cultivation modes for DE.

Table 6.4. Biomass production in domestic effluent during different modes of cultivation.

	Dip **(Hetero)**	***Sce*** **(Hetero)**	***CC*** **(Hetero)**	***Dip*** **(Mixo)**	***Sce*** **(Mixo)**	***CC*** **(Mixo)**
Biomass Concentration (g/L)	4.64±0.2	4.18±0.09	7.97±0.08	6.14±0.03	5.44±0.06	8.87±0.05
Volumetric Biomass Productivity (g/L/day)	0.61±0.03	0.52±0.01	1.11±0.01	0.73±0.01	0.63±0.04	1.24±0.01

Dip and *Sce* represent mono-cultivation mode; *CC* represents co-cultivation mode; Hetero: Heterotrophic mode; Mixo: Mixotrophic mode;

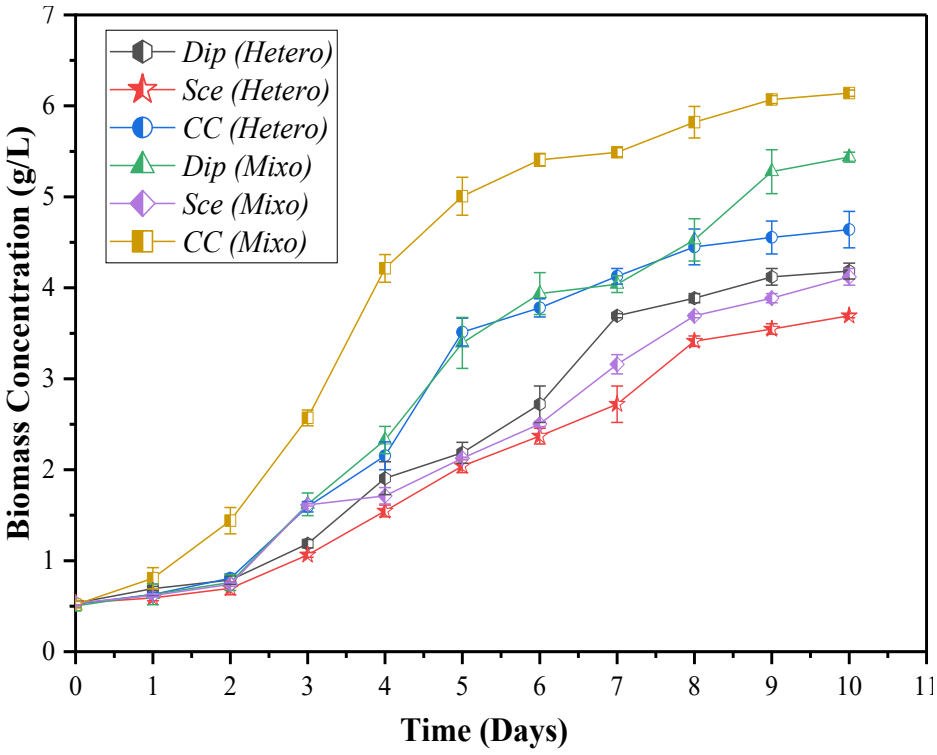

Figure 6.5. The pattern of growth under different modes of cultivation in domestic effluent.

It is visible that the highest biomass productivity was achieved in the co-cultivated mode in comparison to the mono-cultivation mode in both heterotrophic and mixotrophic modes. As per **Figure 6.5,** there was a two-day lag period as no prior acclimatisation of cultures was performed in effluents. During the lag phase, microbes acclimatise themselves to the adverse environment of wastewater through various physiochemical changes, such as the synthesis of enzymes required for the assimilation of substrates present in the medium [377]. The highest biomass concentration and productivity were obtained during the mixotrophic co-cultivation mode, which were 8.87 ± 0.05 g/L and 1.24 ± 0.01 g/L/day, respectively. In mono-cultivation mode, the *D. mucosa* strain performed better than the *S. obliquus* strain, with biomass concentration reaching 6.14 ± 0.03 g/L during mixotrophic cultivation mode and 4.64 ± 0.2 g/L during the autotrophic mode. The reason may be a better adaptation of the *D. mucosa* strain to the wastewater environment. *Diplosphaera* species were first isolated by P.A. Broady from Antarctic terrestrial habitats in 1983 [378].

Due to their source of isolation, *Diplosphaera* species may readily adapt to their environment and the unfavourable characteristics of wastewater. Various reports are available in the literature that have reported the co-culturing of microalgae and bacteria for the treatment of DE [44]–[46], but very scarce information is available that has co-cultivated more than one species of microalgae in DE. Khalekuzzaman et al. (2021) cultivated co-cultures of three microalgal strains (*Chlorella vulgaris, Chlorella sorokiniana,* and *Scenedesmus simris*) in DE wastewater in the anaerobic baffled reactor. According to their findings, the highest biomass concentration was 0.53 g/L during 14 days of cultivation under white light [49]. According to various studies in the literature, the mixotrophic mode has higher biomass productivity than other modes because it can use both organic and inorganic carbon sources [379], [380]. Ramsundar et al. (2017) cultivated *Chlorella sorokiniana* in both mixotrophic and heterotrophic modes in municipal effluent. The highest biomass productivity of 0.714 g/L/day was obtained during the mixotrophic mode of cultivation [105].

The same result was obtained for TE, i.e., the highest biomass productivity was obtained in co-cultivated mixotrophic cultures, as shown in **Table 6.5**. The pattern of growth is shown in **Figure 6.6.**

Table 6.5. Biomass production in textile effluent under different modes of cultivation.

	***Dip* (Hetero)**	***Sce* (Hetero)**	***CC* (Hetero)**	***Dip* (Mixo)**	***Sce* (Mixo)**	***CC* (Mixo)**
Biomass Concentration (g/L)	4.18±0.09	3.69±0.02	4.64±0.20	5.44±0.06	4.12±0.09	6.14±0.03
Volumetric Biomass Productivity (g/L/day)	0.52±0.01	0.45±0.02	0.61±0.03	0.63±0.04	0.49±0.01	0.73±0.01

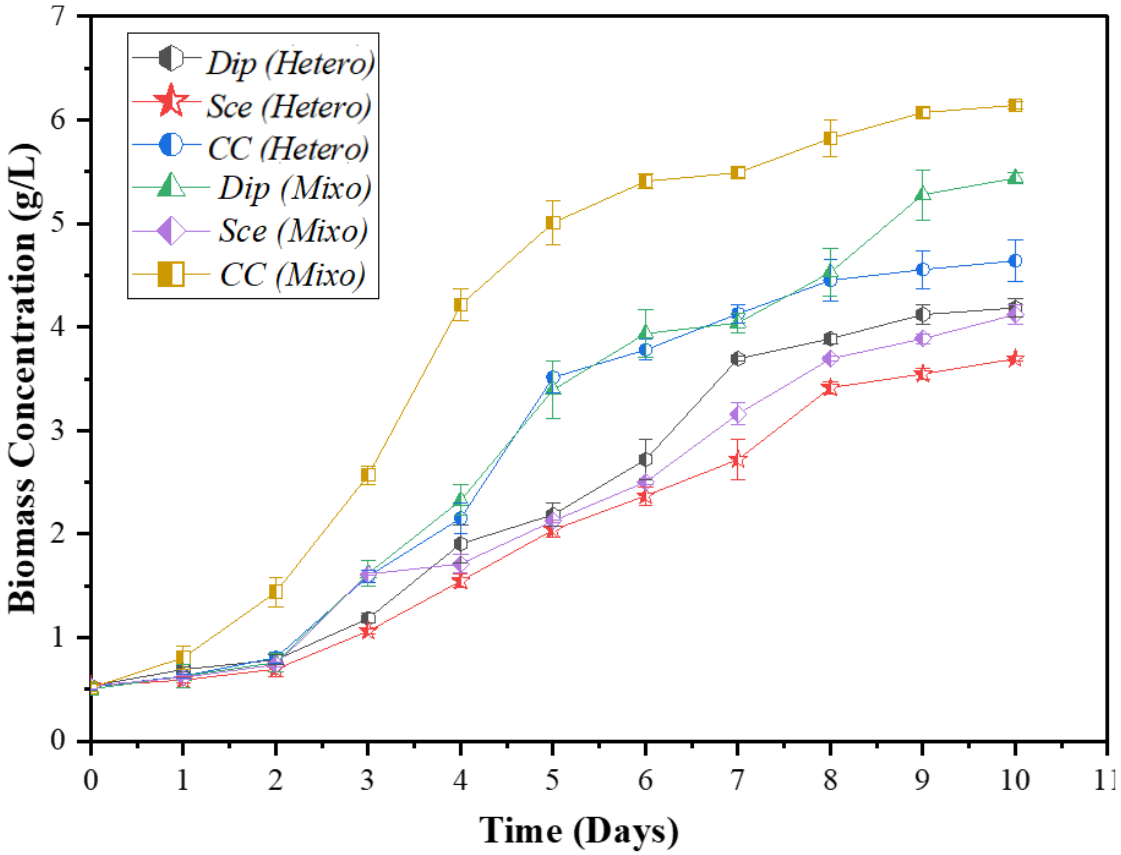

Figure 6.6. The pattern of growth under different modes of cultivation in textile effluent.

In contrast to DE, a three-day log phase was noticed in some cultures, while a stationary phase was obtained in all cultures after eight days. The highest biomass concentration and productivity were obtained in a mixotrophic co-cultivated culture, which were 6.14 ± 0.03 g/L and 0.73 ± 0.01 g/L/day, respectively. Also, during the heterotrophic mode, the highest concentration of biomass and productivity were obtained in the co-cultivation mode, which was 4.64 g/L and 0.61 g/L/day. One of the possible reasons for high biomass productivity in DE in contrast to TE is the nitrogen/phosphorus (N/P) ratio. As per characterization **(Table 6.3),** the N/P ratio of DE was 11.51, while that of TE was 8.6. As the average stochiometric formula of microalgal biomass is $C_{106}H_{181}O_{45}N_{16}P$ based on Redfield's analysis, therefore N/P ratio of the medium should be around 16:1 for high microalgal growth [381]. Similar to the case of DE, authors have focussed more on microalgae-bacterial cultivation for TE [382]–[385]. While very scarce literature is

available, that focuses on the cultivation of more than one microalga species in TE. A mixed microalgae consortium of *Scenedesmus* sp. and *Chlorella* sp. was cultivated via fed-batch operation in TE in a 4.5 L transparent plastic tube PBR. According to the findings, a productivity of 0.49 g/L/d was obtained during the 30 days of the cultivation period after gradual adaptation [386].

6.3.4.2. Pollutant Removal

Various types of pollutants, such as nitrogen, phosphorus, organic carbon, and macro- and micro-elements are present in wastewater. Nitrogen is present in the form of ammonium nitrogen, nitrate, nitrite, organically bound nitrogen, and phosphorus in the form of orthophosphate. These pollutants act as nutrients for microalgal growth, converting them into useful biomass [387]. In the present study, ammonium-nitrogen (NH_4^+-N), phosphate phosphorus (PO_4^{3-}-P), and COD removal have been compared between co-cultivation and mono-cultivation modes in DE and TE. The results were consistent with biomass production, i.e., the highest pollutant removal was achieved in mixotrophic co-cultivation mode.

6.3.4.3. Ammonium Nitrogen Removal Efficiency

NH_4^+-N is the preferential source of nitrogen assimilated by microalgal cells in comparison to nitrate and nitrite, as less energy is required for NH_4^+-N uptake. Microalgae uptake NH_4^+-N through the activity of the ammonium transporter and get it incorporated into glutamine during amino acid synthesis (Sanz-Luque et al., 2015). **Table 6.6** depicts the removal rate and removal efficiency rate of NH_4^+-N from DE, and **Figure 6.7** represents the removal pattern.

Table 6.6. Ammonium nitrogen removal from DE wastewater under different modes of cultivation.

	Dip **(Hetero)**	***Sce*** **(Hetero)**	***CC*** **(Hetero)**	***Dip*** **(Mixo)**	***Sce*** **(Mixo)**	***CC*** **(Mixo)**
Removal Efficiency (%)	87.95±0.45	83.17±0.82	92.01±0.56	91.05±0.23	86.64±0.4	94.57±0.41
Removal Rate (mg/L/day)	10.02±0.2	9.17±0.2	11.17±0.2	10.43±0.01	9.78±0.27	11.6±0.28

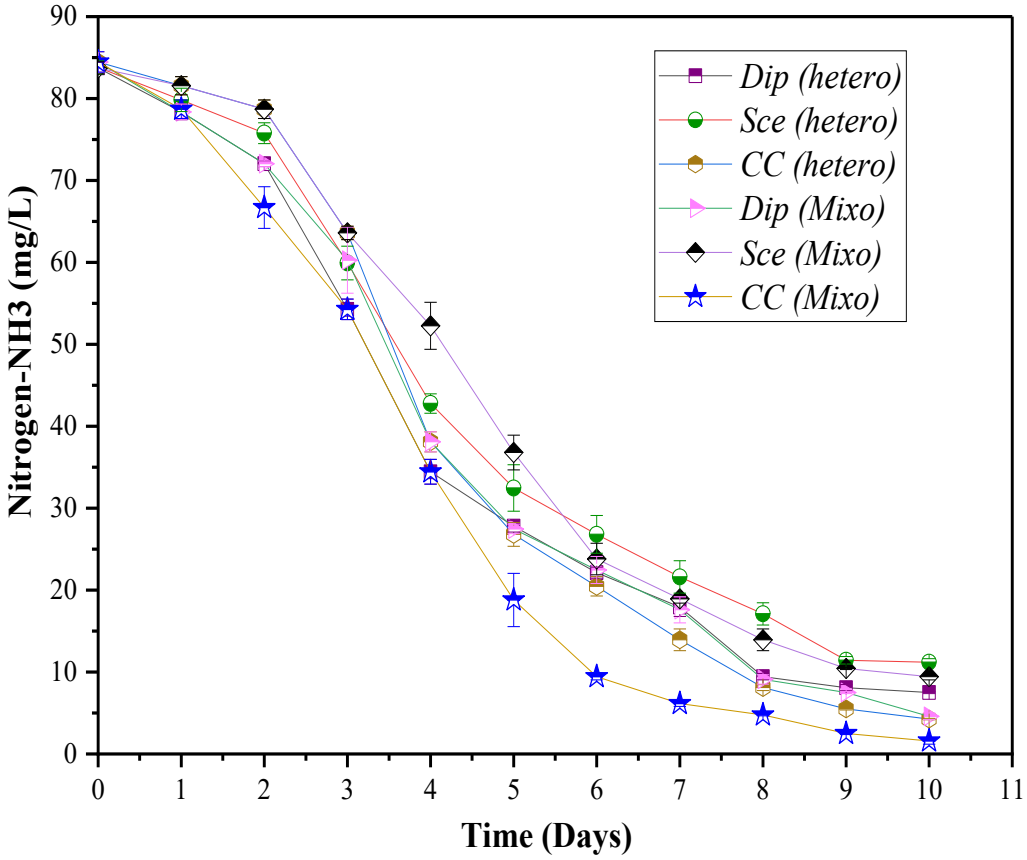

Figure 6.7. The pattern of ammonium nitrogen removal from DE wastewater under different cultivation modes.

As evident from **Table 6.6,** the highest NH_4^+-N removal efficiency of 94.57 ± 0.41% was obtained in the co-cultivation mixotrophic mode. While in heterotrophic co-cultivation mode, removal efficiency reached 92.01 ± 0.56%. As per Figure 8, the nutrient removal rate was low during the first two days of cultivation due to the log phase. But after

that, it drastically increased after the 2nd day and became nearly stable after the 8th day during the stationary phase. The removal efficiency obtained in the present investigation was significantly higher than in the previous study. Two mixed microalgae consortiums entitled MAC1 and MAC2 were cultivated in DE and evaluated for their treatment efficiency [388]. MAC1 consortia dominant with *Nannochloropsis* sp., *Chlorella* sp., *Scenedesmus bijugatus*, *Oscillatoria* sp., and *Chlamydomonas reinhardtii* was able to remove 87 ± 0.50% of NH_4^+-N. While MAC 2 consortia were dominant with *Nannochloropsis* sp., *Chlorella* sp., *Kirchnella*, *Microcoleus*, and *S. dimorphus* removed only 62 ± 0.005% [388].

NH_4^+-N removal from TE is shown in **Table 6.7**, and the pattern of removal is represented in **Figure 6.8.** As expected, the highest NH_4^+-N removal efficiency was obtained during the co-cultivation mixotrophic mode, which was 93.00 ± 0.70% with a 6.6 ± 0.2 mg/L/d removal rate. In heterotrophic co-cultivation mode, NH4+-N removal efficiency was 90.60 ± 0.40% with removal rate of 5.9 ± 0.2 mg/L/d. Here also, the removal rate was low during the first two days of cultivation. After that, the removal rate drastically increased and became stable after the 8th day of the cultivation period, showing synergy with biomass production. The co-cultivation technique can easily surpass other techniques for TE treatment. Wu et al. (2020) used immobilised Chlorella sp. Wu-G23 entrapped inside alginates beads to treat TE. According to their findings, the immobilised strain removed 0.2% of NH_4^+-N (Wu et al., 2021). Even the strains in the current study showed higher removal efficiency than the previous immobilised strain when cultivated in mono-cultivation mode. The *D. mucosa* strain removed 90.2 ± 0.1% and 87.1 ± 0.6% of NH_4^+-N during cultivation in mixotrophic and autotrophic modes, respectively. While the *S. obliquus* strain removed 86.6 ± 0.2% and 84.10 ± 1.00% of NH_4^+-N during cultivation in mixotrophic and autotrophic modes, respectively.

Table 6.7. Ammonium nitrogen removal from textile effluent under different modes of cultivation.

	Dip **(Hetero)**	***Sce*** **(Hetero)**	***CC*** **(Hetero)**	***Dip*** **(Mixo)**	***Sce*** **(Mixo)**	***CC*** **(Mixo)**
Removal Efficiency (%)	87.10±0.60	84.10±1.00	90.60±0.40	90.20±0.10	86.60±0.20	93.00±0.70
Removal Rate (mg/L/day)	6.20±0.10	5.80±0.10	5.90±0.20	6.00±0.20	6.00±0.20	6.60±0.20

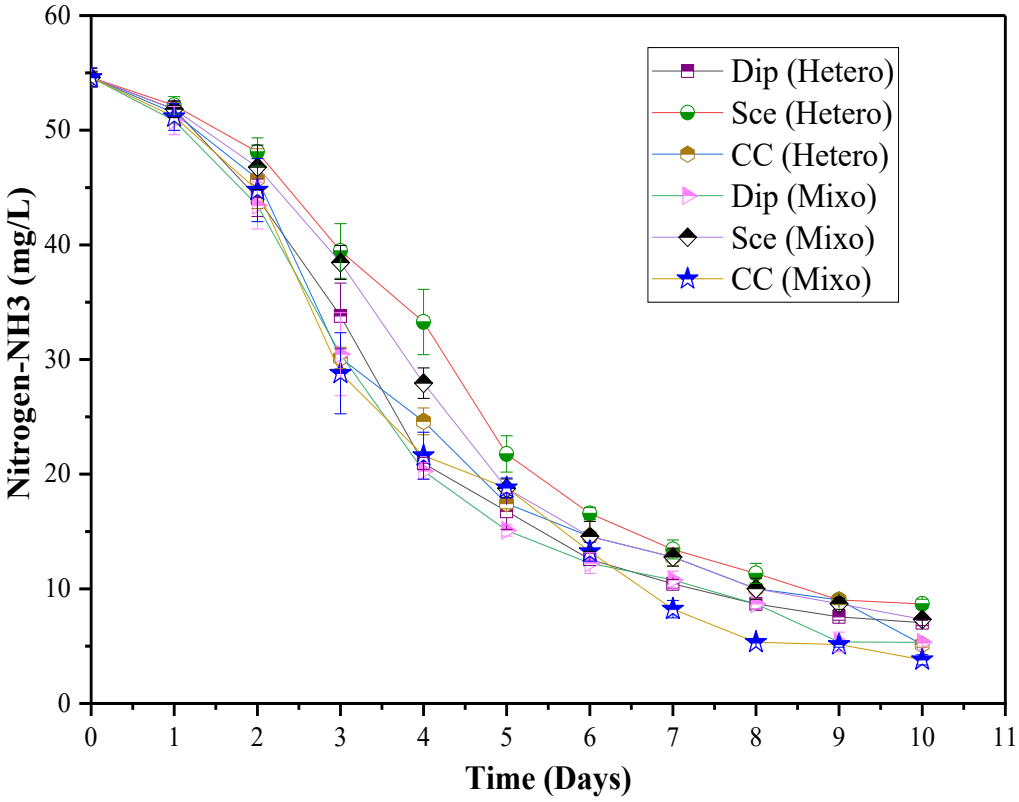

Figure 6.8. The pattern of ammonium nitrogen removal from textile wastewater under different cultivation modes.

6.3.4.4. Phosphate Phosphorus Removal Efficiency

Phosphorus is generally present in the form of orthophosphate (PO_4^{3-}-P) in wastewater, which is introduced into microalgal cells through active transport. Then, via the substrate, oxidative, and photophosphorylation processes, PO_4^{3-}-P is incorporated into various organic compounds such as ATP [347]. Excess PO_4^{3-}-P in the medium is also stored as

polyphosphate granules in the vacuoles of some species. These granules can be utilised later on in phosphorus-deficient conditions [390]. Similar results were also obtained in the case of phosphorus removal (PO_4^{3-}-P), i.e., the highest removal efficiency was obtained in the mixotrophic co-cultivation mode. However, the removal efficiency and rate of PO_4^{3-}-P are lower than those of NH^{4+}-N because microalgae strains require much less phosphorus than nitrogen [22]. **Table 6.8** represents the PO_4^{3-}-P removal efficiency, and **Figure 6.9** represents the pattern of PO_4^{3-}-P removal from DE wastewater.

Table 6.8. Phosphate-phosphorus removal from DE wastewater under different modes of cultivation.

	Dip **(Hetero)**	***Sce*** **(Hetero)**	***CC*** **(Hetero)**	***Dip*** **(Mixo)**	***Sce*** **(Mixo)**	***CC*** **(Mixo)**
Removal Efficiency (%)	71.63±0.9	68.78±1.93	77.29±1.39	74.3±1.26	70.51±0.52	81.59±1.54
Removal Rate (mg/L/day)	0.76±0.03	0.68±0.01	0.82±0.05	0.81±0.03	0.74±0.05	0.69±0.04

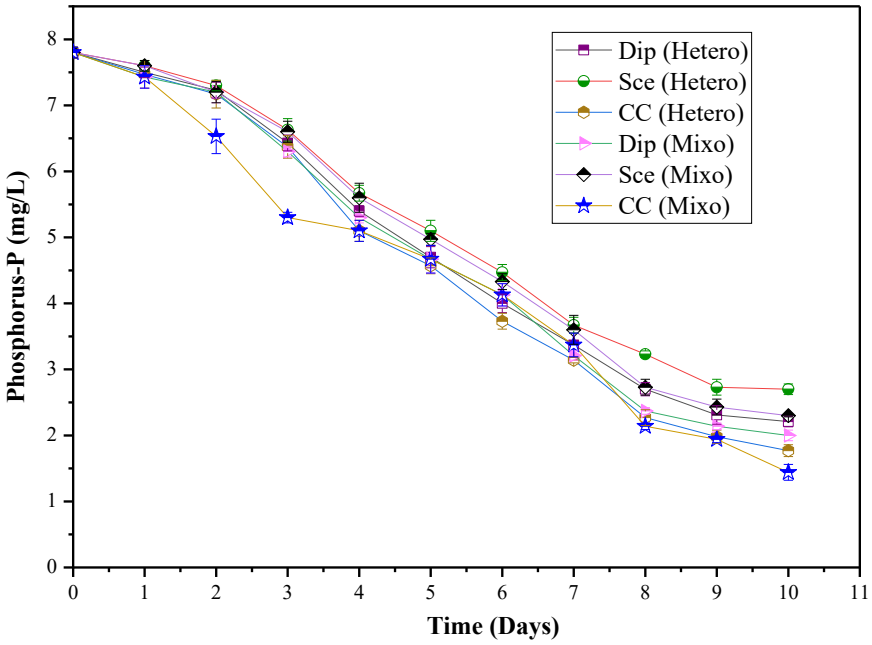

Figure 6.9. The pattern of phosphate phosphorus removal from DE wastewater under different cultivation modes.

The highest removal efficiency of 81.59 ± 1.54% was obtained during the co-cultivation mixotrophic mode, with a removal rate of 0.69 ± 0.04 mg/L/d. While during heterotrophic co-cultivation mode, strains were able to remove 77.29 ± 1.39% of PO_4^{3-}-P with a removal rate of 0.82 ± 0.05 mg/L/d. As per the same pattern as in NH_4^+-N removal, the removal rate of PO_4^{3-}-P was low during the first two days of the cultivation period. After the second day of the cultivation period, the rate drastically increased in the mixotrophic co-cultivation mode, while a slow increase was noticed among other cultivation modes. Stability was achieved after the 8th day, nearly in all cultivation modes. The removal efficiency was greater than that reported in the previous study when co-cultivation was conducted. Barreiro-Vescovo et al. (2021) cultivated a mixed microalgae-bacterial consortium dominated by *Chlorella sorokiniana* in a 1.65 L photobioreactor to treat DE [391]. The consortium removed 68.30 ± 25.2% of PO_4^{3-}P after 23 days of the cultivation period. After some operations, the reactor was dominated by pigmented and photoheterotrophic bacteria, resulting in less microalgal biomass production[391]. Therefore, as mentioned earlier, the consortium of microalgae-bacteria is not suitable for microalgae biomass production in wastewater. Phosphate removal efficiency and rate from TE have been represented in **Table 6.9** and **Figure 6.10.**

Table 6.9. Phosphate-phosphorus removal from textile wastewater under different modes of cultivation.

	Dip **(Hetero)**	***Sce*** **(Hetero)**	***CC*** **(Hetero)**	***Dip*** **(Mixo)**	***Sce*** **(Mixo)**	***CC*** **(Mixo)**
Removal Efficiency (%)	71.60±1.90	66.70±1.00	75.20±0.40	74.70±1.10	70.40±0.70	80.70±1.70
Removal Rate (mg/L/day)	0.60±0.03	0.59±0.01	0.63±0.03	0.60±0.01	0.62±0.04	0.69±0.03

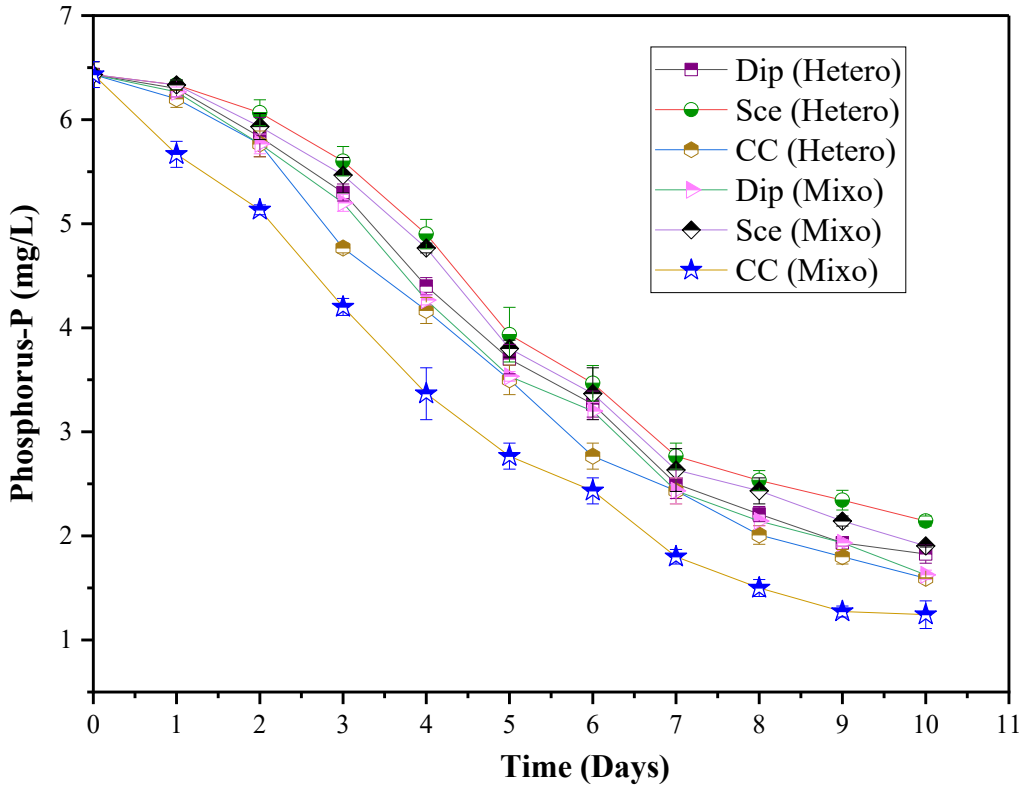

Figure 6.10. The pattern of phosphate phosphorus removal from textile wastewater under different cultivation modes.

With the same removal pattern as in previous cases, the highest PO_4^{3-}-P removal efficiency of 80.70 ± 1.70% was achieved in mixotrophic cultivation mode, with a removal rate of 0.69 ± 0.03 mg/L/d. The heterotrophic mode had a significant removal efficiency of 75.20 ± 0.63% as well. The removal efficiency of the pollutants in the co-cultivation mode can be increased after the gradual adaptation of the strains in TE effluent, as performed by Kumar et al. (2018). They performed a steady acclimatisation of mixed microalgal consortiums of *Chlorella* and *Scenedesmus* sp. in 5 cycles, resulting in the approximate complete removal of total N and P from the effluent [386].

6.3.4.5. COD Removal Efficiency

Another crucial factor in wastewater treatment is chemical oxygen demand (COD), which is a measure of the organic load (strength of the effluent) in the wastewater and the amount of molten oxygen that may be used for its oxidation [392]. In contrast to other common

nutrients like nitrogen and phosphorus, the fate of COD during microalgal-based wastewater treatment processes has not been extensively characterised [393]. Both the strains grown in mono- and co-cultivation modes were able to remove a high percentage of COD from both effluents, indicating that microalgae can assimilate the organic content present in the wastewater with high uptake. In heterotrophic mode, microalgae solely depend upon organic carbon content, while in mixotrophic mode, they can utilise both organic and inorganic carbon content. Inorganic carbon is fixed through a dark reaction and gets transformed into triosephosphate. While organic carbon gets transformed into triose phosphate in the cytosol through various enzymatic reactions and transferred to chloroplast. Triose phosphate is finally transformed into starch or lipid in the chloroplast, depending on the stress condition [387]. COD removal efficiency and rate from DE have been represented in **Table 6.10** and **Figure 6.11.**

Table 6.10. COD removal from domestic effluent under different modes of cultivation.

	Dip **(Hetero)**	***Sce*** **(Hetero)**	***CC*** **(Hetero)**	***Dip*** **(Mixo)**	***Sce*** **(Mixo)**	***CC*** **(Mixo)**
Removal Efficiency (%)	82±0.6	79.6±0.3	87.1±0.5	84.6±0.4	82.1±0.6	90.3±0.5
Removal Rate (mg/L/day)	62.1±1.8	55.9±1.2	65.9±1.8	64.4±1.1	58.1±1.8	67.8±0.8

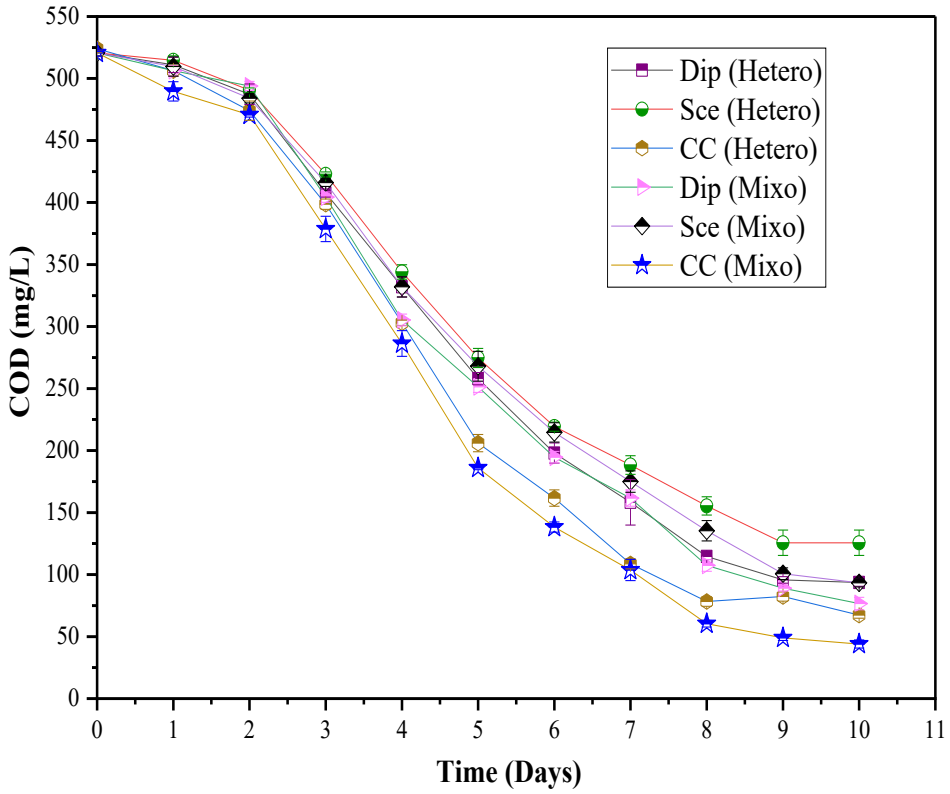

Figure 6.11. The pattern of COD removal from domestic effluent under different cultivation modes.

As per **Figure 6.11**, a drastic decrease in COD from 520.7 ± 2.5 mg/L to 286 ± 10.3 mg/L was obtained after a four-day cultivation period in mixotrophic co-cultivation mode, with a 67.8 mg/L/d removal rate. The final concentration reached 50.70 ± 2.50 mg/L with a removal efficiency of 90.30 ± 0.50%. The heterotrophic co-cultivation mode also indicated better performance, with a removal efficiency of 87.10 ± 0.50%. The co-cultivation technique proved to be more beneficial than the combined process of MFC and microalgae, where a large portion of COD was removed in a microbial fuel cell (MFC) by bacteria [394]. Jiang et al. (2017) treated DE using MFC and column glass PBR combined. The combined process removed 67% of COD after six days of the cultivation period [394]. Next, the results for TE are indicated in **Table 6.11** and **Figure 6.12**.

Table 6.11. COD removal from textile effluent under different modes of cultivation.

	Dip **(Hetero)**	***Sce*** **(Hetero)**	***CC*** **(Hetero)**	***Dip*** **(Mixo)**	***Sce*** **(Mixo)**	***CC*** **(Mixo)**
Removal Efficiency (%)	77.60±0.80	70.80±0.70	83.30±1.50	81.20±0.70	74.40±0.80	86.60±1.10
Removal Rate (mg/L/day)	34.10±0.90	31.80±2.30	36.30±2.40	42.60±0.70	37.40±0.60	44.60±2.40

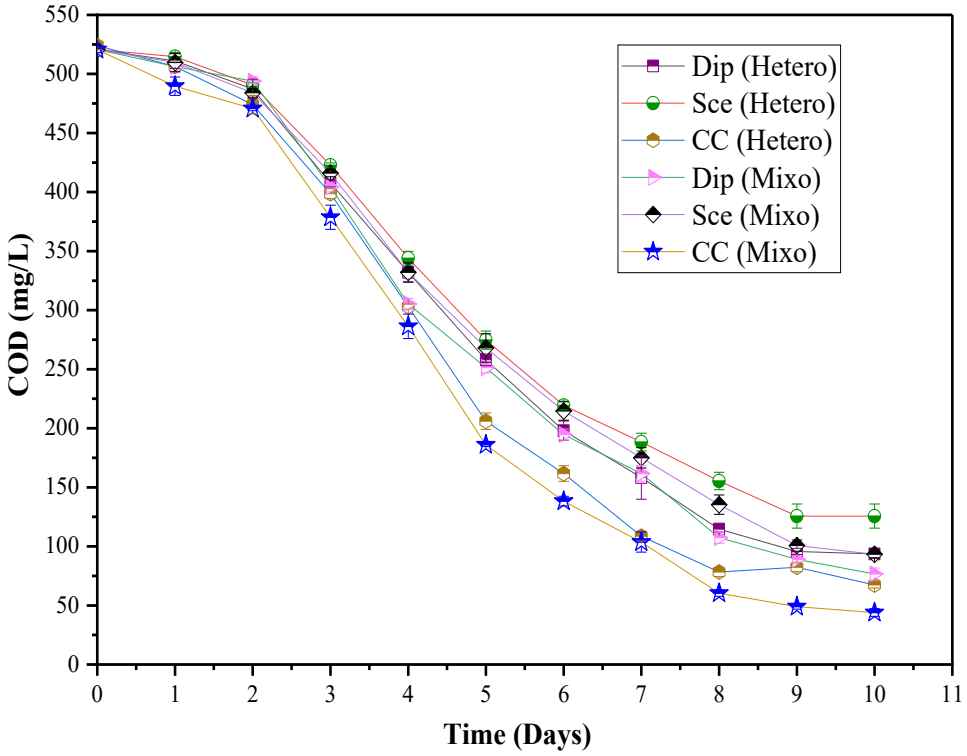

Figure 6.12. The pattern of COD removal from textile effluent under different cultivation modes.

In contrast to DE, a rapid decrease in COD was noticed in the mixotrophic co-cultivation mode just after the first day of the cultivation period. COD declined from 372 mg/L to 260 mg/L, 56.20 mg/L/d removal rate, after the first day of the cultivation period. The final removal efficiency in mixotrophic co-cultivation mode was 86.60 ± 1.10 %, with

a final removal rate of 44.6 ± 2.4 mg/L/d. Strains also performed well in heterotrophic co-cultivation mode, with a final removal efficiency of 83.30 ± 1.50% and a final removal rate of 36.30 ± 2.4 mg/L/d. In this case, the microalgae co-cultivation mode also provided better results than other treatment modes, such as the microalgae-bacteria co-cultivation mode or immobilisation technique. Mubashar et al. (2020) cultivated *Chlorella vulgaris* and *Enterobacter* sp. MN17 at different dilutions of TEs. The highest removal efficiency of COD reached 74% at 5% dilution [395]. Wu et al. (2020) cultivated immobilised strains of *Chlorella vulgaris* G-22 and *Chlorella vulgaris* G-23 at different concentrations of TE. Both strains removed, on average, 50-60% of COD [396].

6.3.5. Model Simulation

As the study was mainly focused on co-cultivation, the model simulation study was conducted using the data obtained during the co-cultivation of microalgal species in DE sewage and TE effluent.

6.3.5.1. Simulation of biomass production models

Results obtained during the model simulation study for biomass production are represented in **Figures 6.13** for TE effluent, respectively. Kinetic parameters are given in **Table 6.12.** Compared to the Gompertz model, the Logistic growth model offered a superior fit for all cases. During Gompertz model simulation, the R^2 value reached 0.94 for both heterotrophic and mixotrophic cultivation. Similarly, in the case of TE, the Logistic model simulated a better fit than the Gompertz model. The better fit of the Logistic model indicates an inverse relationship between the specific growth rate and the current biomass concentration. As the biomass concentration increases, the specific growth rate decreases and tends to zero when the final biomass concentration reaches the maximum carrying capacity of the habitat (K) [397], [398].

Table 6.12. Growth kinetic parameters obtained from logistic and Gompertz model during co-cultivation mode

Wastewater Source	Co-cultivation Mode	Model	Kinetic Parameters	R^2	Adj. R^2	RMSE
		Gompertz	μ_m=1.58 d^{-1}	0.94	0.94	1.15
			λ=1.34 d			
Textile	CC	Logistic	μ_m=0.56 d^{-1}	0.96	0.96	0.86
Effluent	(Hetero)					
		Gompertz	μ_m=0.87 d^{-1}	0.94	0.93	0.80
			λ=1.07 d			
	CC (Mixo)	Logistic	μ_m=0.73 d^{-1}	0.92	0.91	0.64
		Gompertz	μ_m=1.27 d^{-1}	0.90	0.89	0.70
			λ=1.34 d			

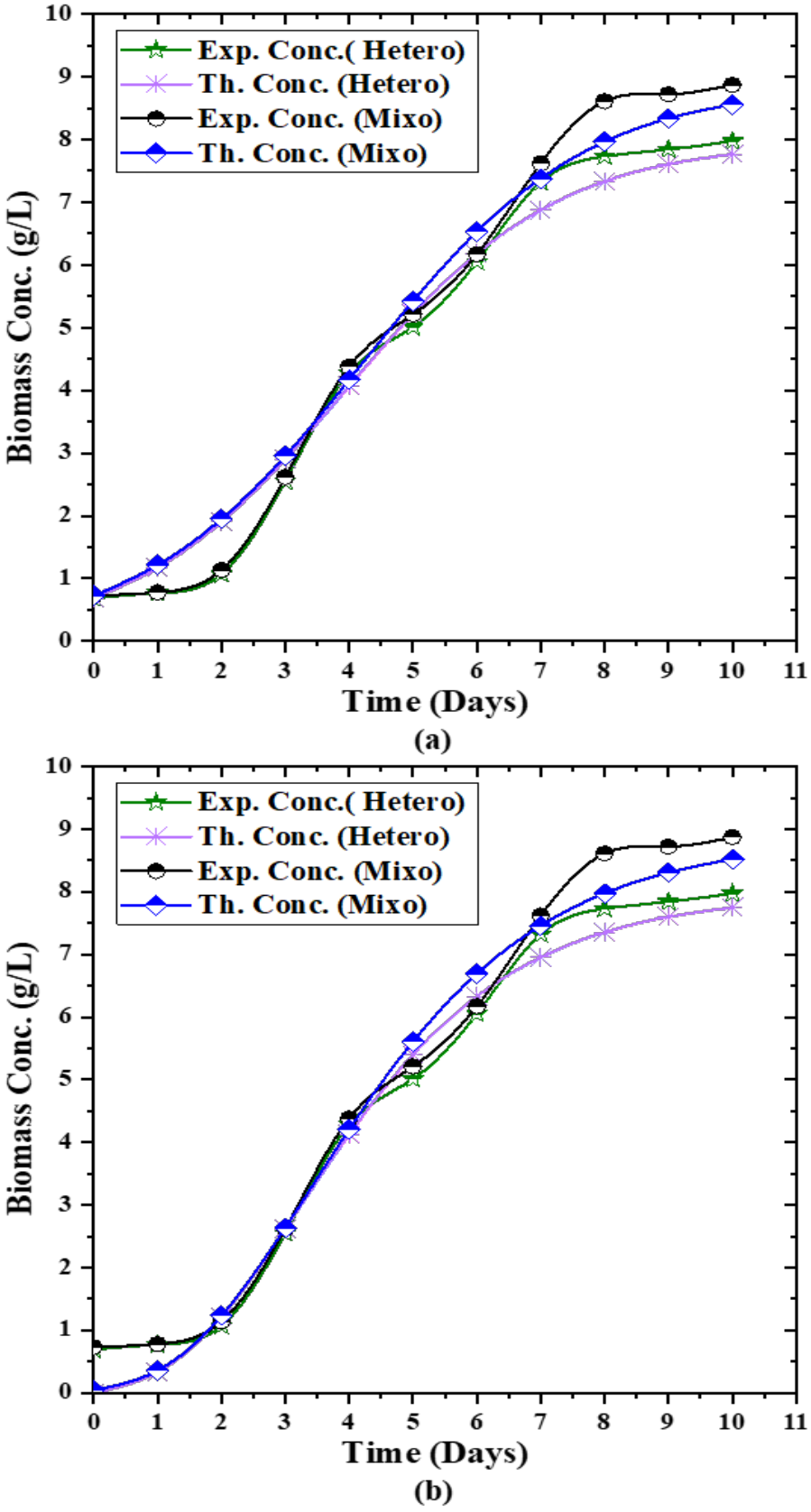

Figure 6.13. Simulation curve for biomass production during cultivation in textile effluent: (a) Logistic Model, (b) Gompertz Model.

6.3.6.2.Simulation of substrate removal models

Models were simulated for both NH_4^+-N and PO_4^{3-}-P removal. Simulation curves are represented in **Figures 6.14** & **6.15** for NH_4^+-N removal and PO_4^{3-}-P removal, respectively. While the kinetic and model evaluation parameters are represented in **Tables 6.13** and **6.14** for NH_4^+-N removal and PO_4^{3-}-P removal, respectively.

Table 6.13. Kinetic parameters obtained for ammonium nitrogen removal from different models during co-cultivation mode.

Wastewater Source	Co-cultivation Mode	Model	Kinetic Parameters	R^2	Adj. R^2	RMSE
Textile Effluent	CC (Hetero)	Model 2 Gompertz	k=0.21 d^{-1} k=0.51 d^{-1} λ=0.78 d	0.92 0.93	0.91 0.92	35.40 6.38
		Luedeking-Piret	1/Y=6.64 mg/g m=0.54 d^{-1}	0.97	0.97	8.85
		Model 1	p=0.55 d^{-1} Y=0.04 g/mg	0.93	0.93	7.20
	CC (Mixo)	Model 2 Gompertz	k=0.23 d^{-1} k=0.55 d^{-1} λ=0.85 d	0.90 0.91	0.89 0.90	14.17 5.92
		Luedeking-Piret	1/Y=5.58 mg/g	0.91	0.90	7.74

		m=0.40 d^{-1}			
	Model 1	p=0.75 d^{-1}	0.94	0.94	12.35
		Y=0.12 g/mg			
	Model 2	k=0.25 d^{-1}	0.89	0.88	15.90

Table 6.14. Kinetic parameters obtained for phosphate phosphorus removal from different models during co-cultivation mode.

Wastewater Source	**Co-cultivation Mode**	**Model**	**Kinetic Parameters**	**R^2**	**Adj. R^2**	**RMSE**
		Model 2	k=0.17 d^{-1}	0.94	0.94	1.90
Textile Effluent	CC (Hetero)	Gompertz	k=0.48 d^{-1} λ=1.36 d	0.95	0.95	0.33
		Luedeking-Piret	1/Y=0.97 mg/g m=0.54 d^{-1}	0.99	0.99	1.01
		Model 1	p=0.61 d^{-1} Y=1.28 g/mg	0.96	0.96	0.31
		Model 2	k=0.19 d^{-1}	0.93	0.92	1.80
	CC (Mixo)	Gompertz	k=0.46 d^{-1} λ=0.56 d	0.94	0.93	0.40
		Luedeking-Piret	1/Y=0.93 mg/g	0.98	0.98	1.18

	m=0 d^{-1}			
Model 1	p=0.52 d^{-1}	0.94	0.93	0.32
	Y=0.43 g/mg			
Model 2	k=0.23 d^{-1}	0.90	0.89	1.31

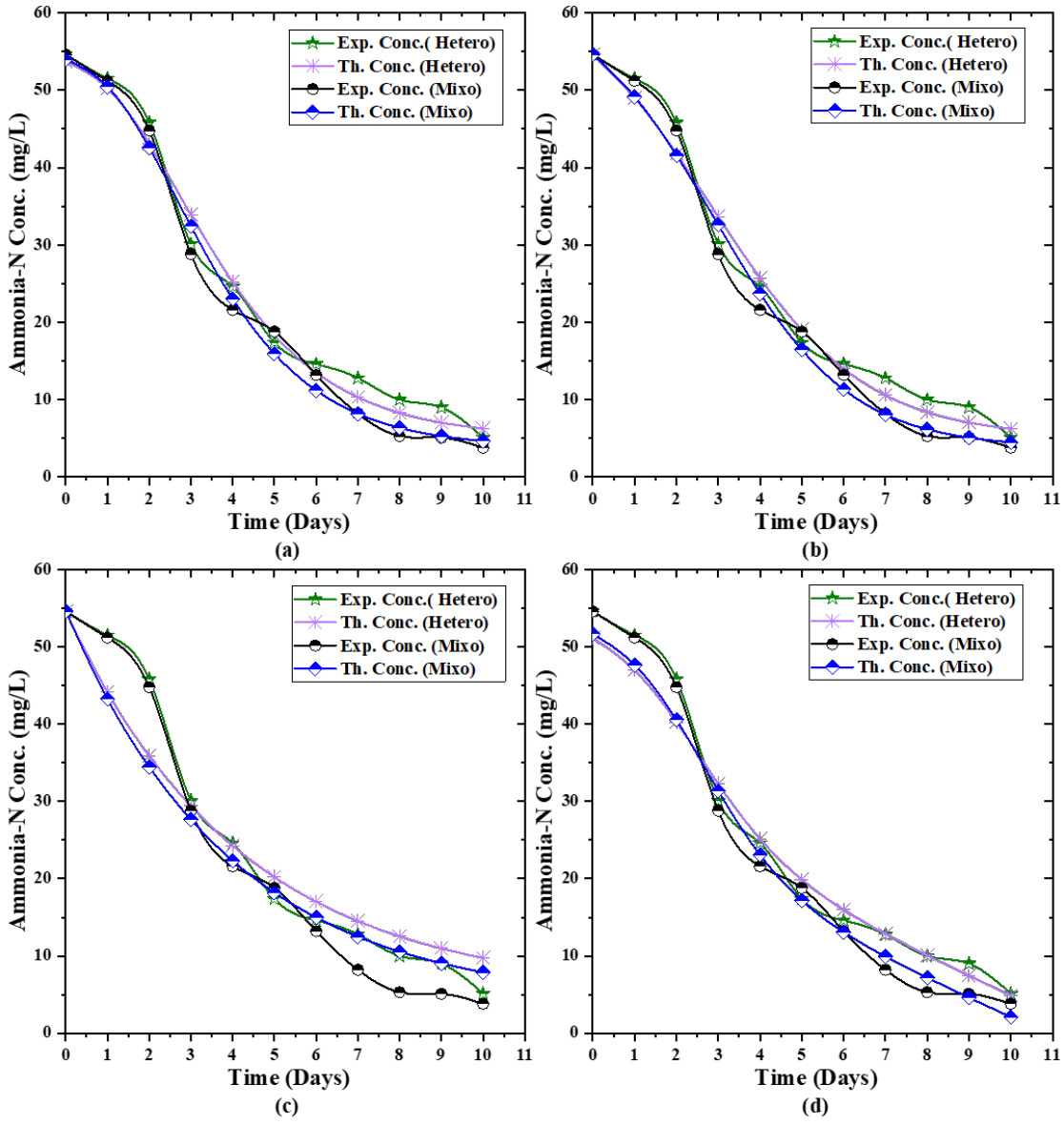

Figure 6.14. Simulation curve for ammonium nitrogen removal from textile effluent: (a) Gompertz Model; (b) Model 1; (c) Model 2; (d) Leudeking-Piret Model.

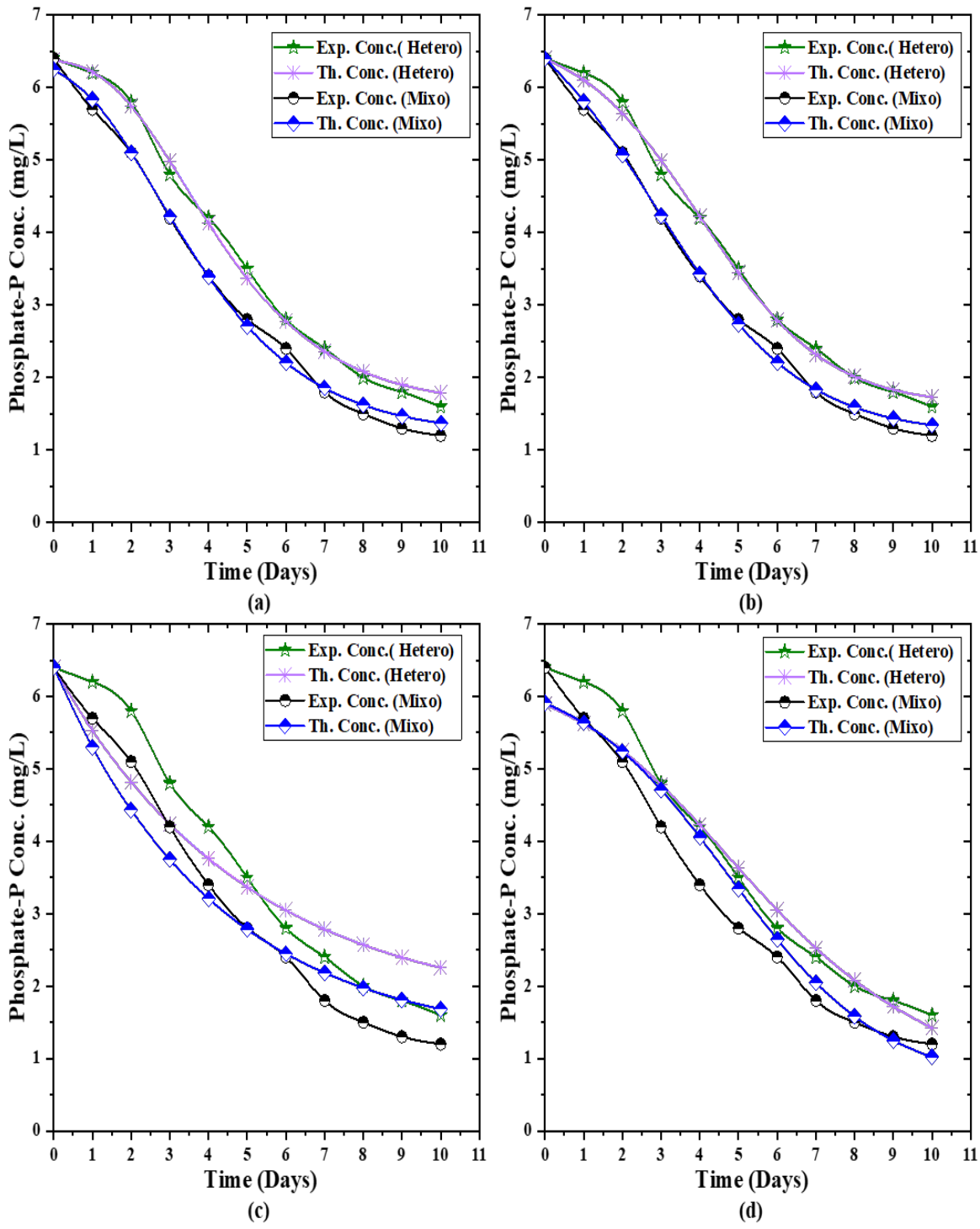

Figure 6.15. Simulation curve for phosphate phosphorus removal from textile effluent: (i) Gompertz Model; (ii) Model 1; (iii) Model 2; (iv) Leudeking-Piret Model.

Results indicated that the Leudeking-Piret model provided a better fit in all cases than other models. Model 1 also offered a better fit than Model 2 and Gompertz. Therefore,

as per the assumptions of these models, substrate removal from wastewater depends on the growth rate of biomass and the existing biomass concentration of microalgae. The Luedeking-Piret coefficient m evaluates the substrate consumed for basic maintenance function. In contrast, 1/Yx in the Luedeking-Piret model determines the capability of cells for substrate consumption during cell growth. The value of Y_x was very high compared to m, indicating that a large amount of substrate was assimilated for biomass production in contrast to maintenance.

6.4. Conclusion

The present study concluded that the symbiotic relationship between two microalgae species could withstand the harsh environment of wastewater, resulting in increases biomass productivity and treatment efficiency. In mixotrophic mode, co-cultivation of *D. mucosa* VSPA and *S. obliquus* resulted in high biomass concentrations of 8.87 g/L in DE and 6.14 g/L in TE. It was also concluded that the mixotrophic mode of cultivation yielded higher biomass productivity than the heterotrophic mode, in both co-cultivation and mono cultivation modes. Pollutant removal was also high in the co-cultivation mixotrophic mode, leading to the 94.57% removal of NH_4^+-N, 81.59% of PO_4^{3-}-P, and 90.3% of COD in DE. While in TE, 93%, 80.70%, and 86.6% removal of NH_4^+-N, PO_4^{3-}-P, and COD, respectively, were obtained. Microscopic and flow cytometry analysis revealed that the co-culture was dominated by the *D. mucosa* VSPA strain due to its high growth rate. At last, the modelling study concluded that the Logistic model for growth and the Leudeking-Piret model for substrate removal better simulated the experimental results. These models can assist in the scale-up of the co-cultivation strategy by predicting important biological parameters such as specific growth rate, lag duration, and maximum biomass concentration. Owing to various advantages, a deeper study on this co-cultivation strategy can be carried out by testing it on more toxic industrial effluents and evaluating more rare strains.